Available online at www.sciencedirect.com

SciVerse ScienceDirect

Ceramics International 39 (2013) 3113–3119

CERAMICS INTERNATIONAL

www.elsevier.com/locate/ceramint

Oxidation kinetics of hot-pressed ZrB_2–SiC ceramic matrix composites

Dong Gao[a,b], Yue Zhang[a,*], Chunlai Xu[c], Yang Song[c], Xiaobin Shi[c]

[a]*Key Laboratory of Aerospace Materials and Performance (Ministry of Education), School of Materials Science and Engineering, Beihang University, Beijing, 100191, PR China*

[b]*AVIC Commercial Aircraft Engine CO., LTD, Shanghai, 200241, PR China*

[c]*National Key Laboratory of Advanced Functional Composite Materials Technology, Beijing, 100076, PR China*

Received 8 July 2012; received in revised form 26 September 2012; accepted 26 September 2012
Available online 3 October 2012

Abstract

The isothermal oxidation of ZrB_2 ceramics with different content of SiC was carried out in air up to 1700 °C, and the effect of chemical composition on the oxidation kinetics of ZrB_2–SiC ceramics was analyzed. As indicated by the experimental results, both ceramics with 20 vol% and 30 vol% SiC particles followed near parabolic oxidation kinetics. And higher concentration of SiC led to better oxidation resistance performance due to the formation of more silica glass on the surface of the specimens and formation of zircon phase $ZrSiO_4$. In addition, the oxidation of the ceramic composites is diffusion controlled and the activation energies for the diffusion of oxygen in the oxide scale of the ceramics oxidized at temperatures below 1500 °C were 5134 J/mol and 5960 J/mol for ZS2 and ZS3, respectively. Then the oxidation of the ceramics transformed to reaction controlled under elevated temperature due to evaporation of the protective silica glass. Furthermore, the evolution process of the surface morphology and oxide scale of the ceramic during initial oxidation stage was given detailed investigation.

Keywords: C. Corrosion; Ceramic matrix composites (CMCs); Scanning electron microscopy (SEM)

1. Introduction

Ceramics with melting points of more than 3000 °C are defined as ultra-high temperature ceramics (UHTCs) [1,2]. Borides, nitrides and carbides of transitional metals are typical UHTCs, which are considered as potential candidate material of Thermal Protective System (TPS) for re-entry aircrafts and supersonic vehicles because of their unique combination of high melting points, good thermal shock resistance, and excellent ablation/ oxidation resistance [3–6]. Of those UHTCs, ZrB_2 is considered as most promising material due to its relatively lower density (6.09 g/cm^3). Particularly, the thermal shock resistance property of the ZrB_2 ceramics is superior to other ultra-high temperature ceramics due to its higher thermal conductivity (65–135 W/ (m K)$^{-1}$) [7,8].

However, poor oxidation resistance above 1100 °C generally restricts the widespread application of monolithic ZrB_2 materials [9,10]. As reported in many investigations, the introduction of second phase particles (such as $MoSi_2$, SiC and so on) has succeeded in improving the oxidation resistance performance of the ceramic by forming continuous and protective silicate glass on the surface of the ceramic composites, which inhibits diffusion of oxygen into the inner part of the ceramics [11,12]. And SiC is considered as the most promising second phase introduced to the ceramic due to its relative low density, excellent high temperature properties and better oxidation resistance performance [13]. The oxidation of ZrB_2–SiC ceramics has been studied by a number of investigators and much progress has been obtained. As reported by Alireza Rezaie et al., the oxidation process of ZrB_2–SiC ceramics in air can be divided into three temperature ranges according to evolution of oxidation layer [14]. (I) Below 1200 °C, a protective borate glass layer can be observed from the surface; (II) At 1200 °C and above, the B_2O_3 evaporates and silica rich glass that formed is stable up to at least 1500 °C. Beneath the surface, the oxidation layer consists of porous zirconia layer and SiC depleted layer. (III) At

*Corresponding author. Tel.: +86 10 82316976.
E-mail address: zhangy@buaa.edu.cn (Y. Zhang).

0272-8842/$ - see front matter © 2012 Elsevier Ltd and Techna Group S.r.l. All rights reserved.
http://dx.doi.org/10.1016/j.ceramint.2012.09.091

temperatures above 1500 °C, silica glass evaporates and the oxidation layer consists of columnar zirconia, which has poor oxidation resistance performance [14]. Furthermore, low oxygen partial pressure leads to even more serious oxidation due to active oxidation of SiC under relatively low temperature in comparison to the material oxidized in air, which results in the formation of SiC depleted layer. Additionally, a thermodynamic model has been set up in order to understand the evolution of the oxide scale during oxidation process. In the proposed model, the formation of SiC depleted layer was analyzed with the help of the volatility diagram of ZrB_2–SiC system [15]. Although several oxidation kinetics models have been proposed by many investigators, while almost all of them focused on the interpretation of the oxidation process according to the TG curves and the detailed information about oxidation process is still not clearly understood. For example, Parthasarathy et al. proposed an oxidation model of SiC containing diborides in the temperature range of 1000–1800 °C, which given thoroughly investigation to the oxygen diffusion and evaporation of borate glass during oxidation at elevated temperatures [16]. However, the activation energy with practical meaning about the oxidation process cannot be obtained. In addition, many investigations have confirmed that the oxidation of the SiC containing boride ceramic composites is diffusion controlled at intermediate high temperatures according to the TG curves, while energy barrier for the diffusion process in unclearly known [17,18].

In the present work, ZrB_2 ceramics with different chemical composition were oxidized in air with the purpose of clarifying the oxidation kinetics of the material, and Chou's model was employed which had succeeded in clarifying oxidation kinetics of many refractory materials. The effect of chemical composition on the oxidation process was given special consideration. Furthermore, the evolution of surface morphology of the material in initial oxidation was clarified according to experimental results.

2. Experimental procedure

2.1. Material processing

Commercially available ZrB_2, and SiC powders with a reported purity of 99% and an average particle size of 2 um were used. ZrB_2 based ceramic composites with 20 vol% and 30 vol% were prepared by the hot pressing method, and they were abbreviated as ZS2 and ZS3 in the following discussion. The detailed preparation process has been described in previous research [19]. Sample coupons in the size of 10 mm × 10 mm × 5 mm were cut from sintered materials by the electrical discharge machining (EDM) method, and all the surface of the specimens was diamond polished to 1 μm finish. The coupons were ultrasonically cleaned successively in deionized water and ethanol before oxidation test.

2.2. Oxidation test

The oxidation process was conducted in a tabular furnace with molybdenum disilicide ($MoSi_2$) heating elements capable of operating at 1800 °C. Both of ZS2 and ZS3 were oxidized in air at 1200 °C, 1300 °C, 1400 °C and 1500 °C. The ceramics were put into the center of the alumina tube when reaching the targeted temperatures and then put out from the tube after oxidation for different holding time. In the present work, the ceramics were oxidized in air up to 90 min. Then the weight of oxidized specimens was measured immediately after oxidation by an analytical balance which has a resolution of 0.1 mg, thus the weight changes of the ceramics with variation of holding time can be obtained. Furthermore, the ZS2 ceramics were oxidized at 1700 °C in air up to 90 min with the purpose of clarify oxidation behavior of the ceramic at elevated temperatures.

2.3. Characterization of oxidized specimens

Crystalline phases of oxidation products were determined by X-ray diffraction (XRD, Dmax-2200, Rigaku, Tokyo, Japan) with Cu Ka radiation. The morphology and chemical composition of oxidation products on the surface and oxidation layer was detected by an Electronic Scanning Microscopy (Camscan3400, Oxford, England) which equipped with an EDS detector (INCAINCAPentaFET-x3, Oxford, England).

3. Results and discussion

3.1. Evolution of oxidized surface

The oxidized surface of ZS2 ceramic, exposed to 1500 °C in air with increasing of holding time, was studied using XRD, SEM and EDS. Thus the evolution of oxidized surface can be identified. Fig. 1 shows the XRD patterns of ZS2 ceramics oxidized in air for different holding time.

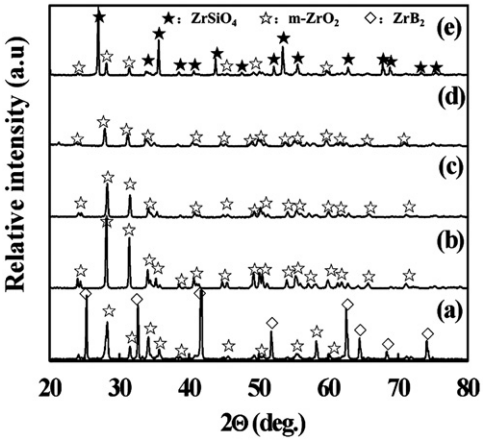

Fig. 1. XRD patterns of ZS2 ceramics after oxidation under 1500 °C, (a) 1 min, (b) 10 min, (c) 30 min, (d) 60 min and (e) 90 min.

As shown in the image, most of the ZrB_2 is unaffected after oxidation for 1 min, and about 33.2 wt% monolithic zirconia can be identified from the XRD pattern according to the quantitative analysis result while the formation boron oxide and silica glass cannot be identified. After oxidation in air for 10 min, oxidation products consist of zirconia crystals and amorphous borate silicate glass, and the latter cannot be identified from the XRD pattern, as shown in Fig. 1(b). Then the relative intensity of zirconia decreases with extension of holding time, which implies that more borate silicate glass is formed. It should be noted that zircon phase $ZrSiO_4$ is detected from the oxidation products when oxidation was done in air for 90 min. The formation mechanism of zircon has been clarified in previous investigation [19]. And the formation of zircon is related to the active oxidation of SiC. Furthermore, zircon is also detected from the XRD pattern of ZS3 ceramics oxidized in air for 60 min and 90 min (not shown here), and more zircons have been obtained with higher content of SiC in comparison to that of ZS2 oxidized under the same condition.

The surface morphology of oxidized specimens can be observed from Fig. 2. As shown in Fig. 2(a), the oxidation of ZS2 ceramics in the initial 1 min is slight and only a little oxides can be identified from the surface. More silica glass can be observed from the surface of specimens with extension of holding time due to passive oxidation of SiC. In addition, the oxidation of the ceramic leads to volumetric expansion, which extrudes the liquid glass from the inner part to the surface, thus the surface of the specimen is covered by liquid glass, as shown in Fig. 2(b) and (c). After oxidation at 1500 °C for 30 min, the surface of the ceramics is covered by honeycomb like zirconia particles, and the glass fills the gaps between zirconia particles. The mean size of the zirconia particles reaches to about 30 μm (as shown in Fig. 2(d)). In the further oxidation process, zircon phase $ZrSiO_4$ particles are observed due to active oxidation of SiC, as reported in our previous research [19]. The typical morphology of the zircon phase $ZrSiO_4$ formed after oxidation is shown in Fig. 3. When oxidized under temperatures higher than 1600 °C, the surface of the ceramic is covered by dense zirconia layer due to the extensive evaporation of silica glass, which has been confirmed by Halloran et al. [20]. A typical morphology can be observed from Fig. 4, and the ZS2 ceramic was oxidized under 1700 °C for 30 min.

3.2. Evolution of oxidation layer

As confirmed by previous investigation, the oxidation layer can be divided into three layers when oxidation under temperatures below 1800 °C in air: (I) borate silicate glass; (II) porous zirconia layer and (III) SiC depleted layer. Furthermore, the chemical composition has significant effect on the evolution of oxidation layer, as reported by Han et al. [11]. Fig. 5 shows the backscattered electron image of ZS2 ceramics after oxidation at 1500 °C for 30 min, and the microstructure of the oxide scale can be observed. In addition, the elemental distribution mapping results of Zr, B, Si, C and O on the cross section after oxidation are shown; thus the thickens of oxide scale, silica glass layer and SiC depleted layer can be measured accurately. As shown in the image, after oxidation in air for 30 min, the protective glass layer has been formed for

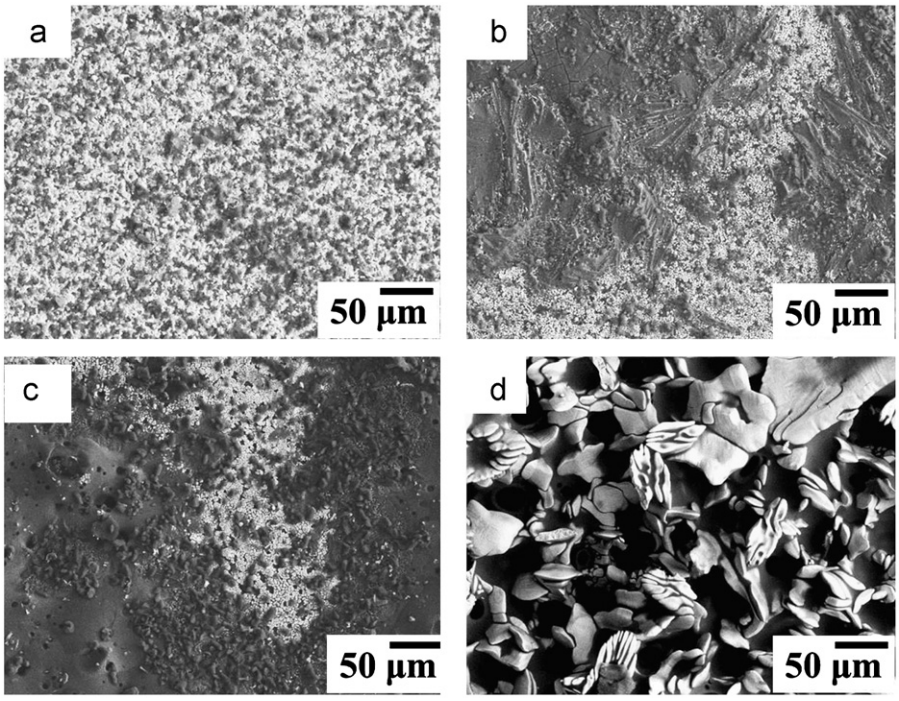

Fig. 2. Surface morphology of ZS2 ceramics after oxidation under 1500 °C in air (a) 1 min, (b) 2 min, (c) 5 min and (d) 30 min.

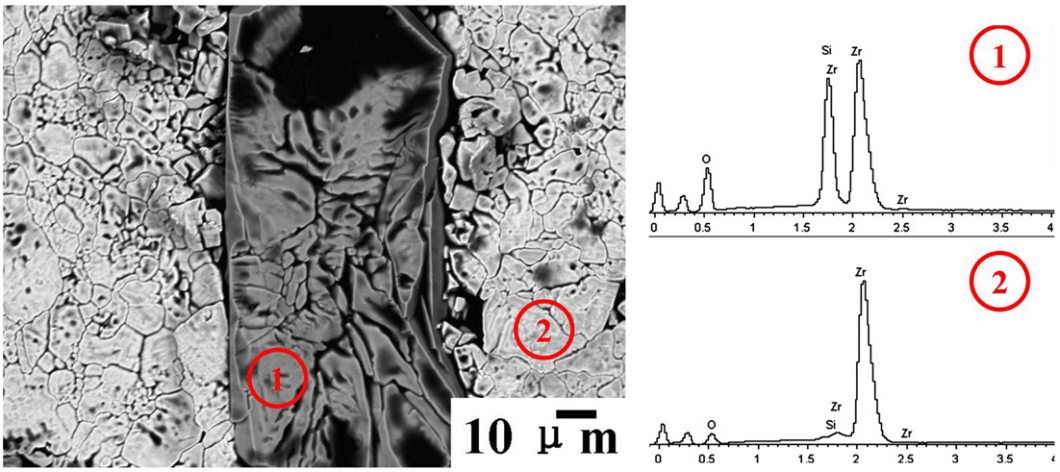

Fig. 3. Zircon phase formed after oxidation under 1500 °C for 90 min, (a) morphology of the oxidized surface and (b) elemental analysis results to the oxidized surface.

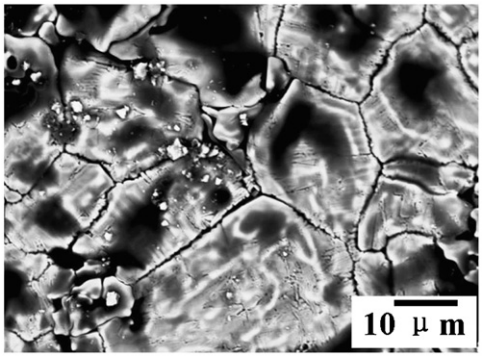

Fig. 4. Surface morphology of ZS2 ceramics oxidized under 1700 °C for 30 min.

ZS2. Furthermore, as indicated by the EDS mapping results, the thickness of oxide scale reaches about 90 μm with a layer of protective glass layer of 15 μm.

The variation of thickness of oxidation layer, silicate glass layer and SiC depleted layer for ZrB_2 based ceramics when oxidation at 1500 °C is shown in Fig. 6 according to the SEM images and EDS mapping results. As shown in the image, during the initial 10 min, the thickness of all the three layers of ZS3 is larger than that of ZS2. However, the glass layer is not continuous due to high viscosity aroused by the passive oxidation of SiC. Hence ZS3 ceramics need longer holding time to obtain the protective layer of silica rich glass in comparison to ZS2. Furthermore, the variation of oxide scale, silica layer and SiC depleted layer of ZS2 and ZS3 show similar increasing trend in the first 60 min, and the thickness of all the layers of ZS3 is smaller than that of ZS2 with the formation of dense and continuous silica rich layer. The difference of variation of oxidation layer between the initial oxidation and further oxidation can be ascribed to the concentration of boron oxide in the silica rich glass, which is evaporative and has higher oxygen diffusivity, as confirmed by Li et al. [21]. It should be noted that all the three layers of ZS2 keep growing after oxidation for 60 min while the oxide scale and SiC depleted layer of ZS3 shows a tendency of decrease, which is aroused by the crystal growth of zircon phase $ZrSiO_4$. As reported in our previous research, the crystal growth of zircon is accompanied by volumetric shrinkage. Then the oxidation resistance performance of the ZS3 ceramics is improved due to lower oxygen diffusion rate through the continuous zircon layer in comparison to that of zirconia. As for ZS2 ceramics, zircon on the surface is not continuous and the surface of the ceramic is mainly covered by monolithic zirconia. ZrO_2 is an n-type oxide, which exhibit both zirconium interstitial ions and oxygen vacancies. Due to such defect structure, ZrO_2 is prone to oxidation by diffusion of both cations as well as anions. Hence the oxidation resistance of the ceramic is deteriorated.

3.3. Oxidation kinetics of ZrB_2-SiC ceramic composites

Cuboid shape specimens were employed in the oxidation test, thus the oxidation kinetics parameters can be obtained according to Chou's model [22,23]. The relation between reacted fraction and holding time is described in Eqs. (1) and (2), where ξ is the oxidized fraction, ΔE is the activation energy for the diffusion of oxygen, v_m is a constant related to the density of substance and oxide, $D_0^0$is the diffusion coefficient of oxygen in the oxide scale, $P_{O_2}$and $P_{O_2}^{eq}$ are the oxygen partial pressure of the environment and the interface between oxide and the unaffected part, while L_0, W_0 and H_0 are the length, width and height of the cuboid specimens, respectively. The detailed derivation process of the equation can be obtained from reference [20,24]. The value of the reacted fraction of the ceramics can be obtained according to the weight gains after oxidation and the reactions during oxidation. In the present case, the oxidation process can be described as Eqs. (3) and (4), and boron oxide is thought to be exhausted due to evaporation. Thus weight changes aroused by oxidation of ZS2 and ZS3 can be deduced according to Eqs. (3) and (4),

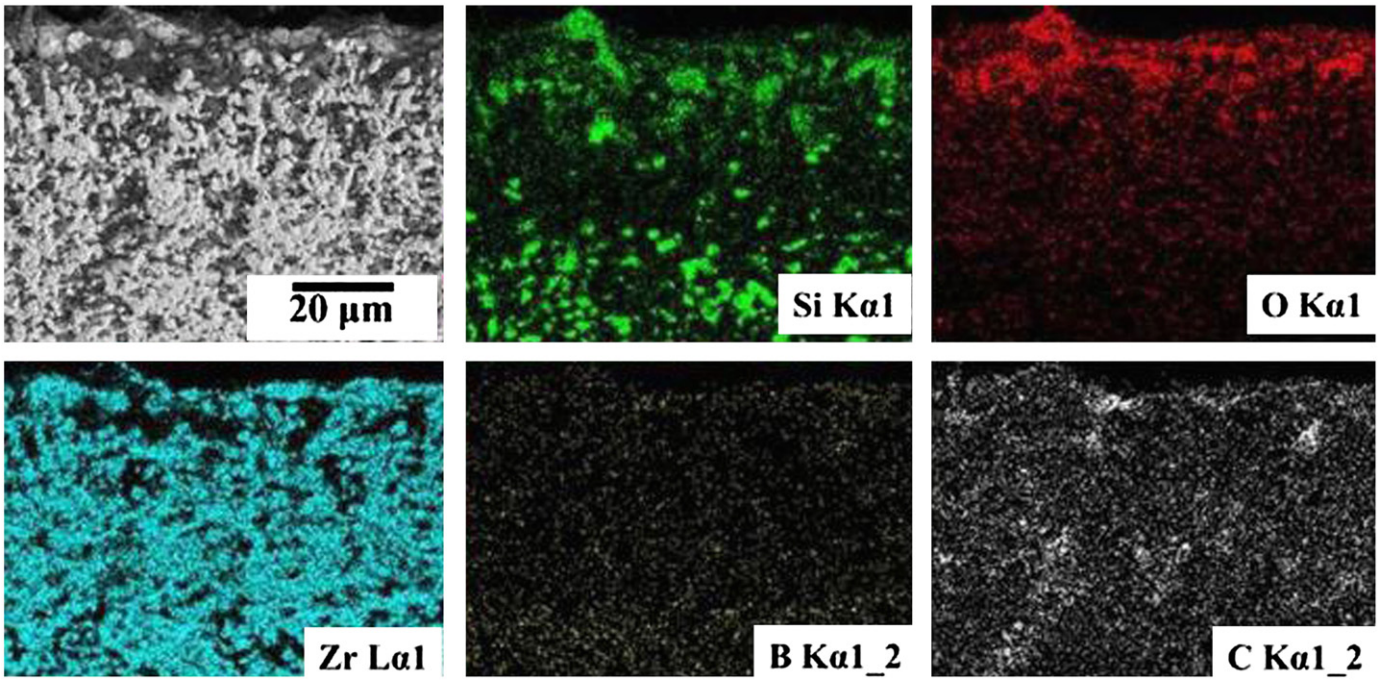

Fig. 5. Microstructure and elemental distribution of the oxide scale for ZS2 ceramic oxidized under 1500 °C for 30 min.

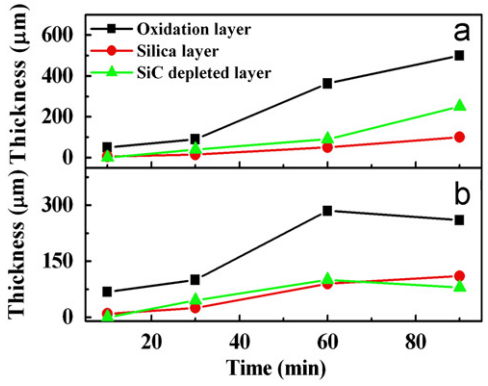

Fig. 6. Variation of the thickness of oxide scale, silica glass layer and SiC depleted layer as a function of holding time when oxidation under 1500 °C, (a) ZS2 and (b) ZS3.

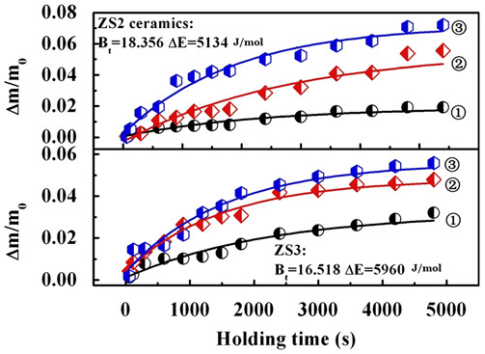

Fig. 7. Comparison plots of from Chou's model and experimental data from isothermal oxidation of ZS2 and ZS3 ceramics in air.

which are 0.139319/g and 0.16691/g, respectively. Then the reacted fraction ξ can be obtained.

$$\xi = 1-\left[1-\frac{2}{L_0}\sqrt{\frac{t}{B_t\exp(\Delta E/RT)}}\right] \times\left[1-\frac{2}{W_0}\sqrt{\frac{t}{B_t\exp(\Delta E/RT)}}\right] \times\left[1-\frac{2}{H_0}\sqrt{\frac{t}{B_t\exp(\Delta E/RT)}}\right] \quad (1)$$

And the variable B_t is defined as

$$B_t = \frac{v_m}{2D_0^0\left(\sqrt{P_{O_2}}-\sqrt{P_{O_2}^{eq}}\right)} \quad (2)$$

$$ZrB_2(cr)+\frac{5}{2}O(g)\rightarrow ZrO_2(cr)+B_2O_3(g) \quad (3)$$

$$SiC(cr)+\frac{3}{2}O_2(g)\rightarrow SiO_2(l)+CO(g) \quad (4)$$

The relation between reacted fraction ξ and holding time for ZS2 and ZS3 ceramics can be identified from Fig. 7. As shown in the image, the oxidation behavior of the ZrB_2–SiC ceramics is significantly affected by the content of SiC. As shown in the image, the value of reacted fraction ξ of ZS2 is larger than that of ZS3 when oxidized under same temperatures, which indicates that the higher content of SiC is beneficial to improving the oxidation resistance performance of the ceramic composites. The improvement of oxidation resistance performance aroused by more SiC can be ascribed to the formation of more silica glass and zircon phase $ZrSiO_4$. In addition, the diffusion energy of oxygen in oxide scale can be obtained according to Eq. (1), as shown in Fig. 7, i.e.,

$\Delta E_{O,\,ZS2} = 5134$ J/mol and $\Delta E_{O,ZS3} = 5960$ J/mol. As indicated by the values of diffusion energy obtained, the diffusion of oxygen in the oxide scale of ZS2 is easier due to a lower diffusion barrier, which results in more serious oxidation. The difference of the diffusion energy aroused by chemical composition of the ceramic composites can be attributed to more silica glass formed on the surface of the ceramics during oxidation process, as indicated by the computation results offered by Li et al. [21]. In addition, the average error, Δ, can be obtained according to Eq. (4). As indicated by the calculation results, the average error is $\Delta = 0.93\%$ and 0.88%, respectively. Thus this is a very good prediction [25].

$$\Delta = \frac{1}{N}\sum_{i=1}^{N}\frac{|(\xi_i)_{mea} - (\xi_i)_{cal}|}{|(\xi_i)_{mea}|}100\% \quad (4)$$

where $(\xi_i)_{mea}$ and $(\xi_i)_{mea}$ refer to the transformed fractions of the measured and calculated values at a fixed time 't', respectively, and N is the total data points.

But with the oxidation condition increasing to temperatures above 1500 °C, the evaporation of silica glass should be given consideration. Thus the oxidation of SiC should follow Eqs. (5) and (6). The weight gain per unit surface area ($\Delta W/S$) of ZS2 oxidized under 1700 °C is shown in Fig. 8. As shown in the image, the $\Delta W/S$ of ZS2 ceramic composite basically follows a linear relation to the holding time when oxidation under 1700 °C and the $\Delta W/S$ of the specimen decreases at a loss rate of -0.908 mg/(cm^2 min). The variation trend of $\Delta W/S$ indicates that the oxidation of the ceramic at elevated temperatures is reaction controlled, and the oxidation should be complete following expression (5) and (6). The decay of oxidation resistance performance of the ceramic can be deduced to the evaporation of liquid silica glass, which is caused by a sharp increase of vapor pressure. Thus the oxidation of the ceramic continues until completely oxidized.

$$SiC(cr) + \frac{3}{2}O_2(g) \rightarrow SiO_2(l) + CO(g) \quad (5)$$

$$SiO_2(l) \rightarrow SiO_2(g) \quad (6)$$

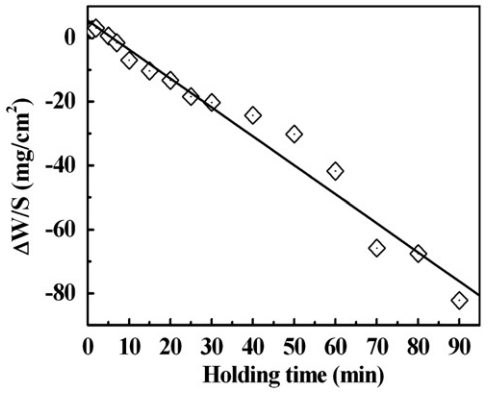

Fig. 8. Variation of weight gain per unit surface area for ZS2 ceramics oxidized under 1700 °C.

4. Conclusion

ZrB_2 ceramics containing 20 vol% and 30 vol% SiC were prepared by hot-pressing method, and the oxidation kinetics of the ceramics was analyzed according to experimental results. Oxidation temperature has an obvious effect on the oxidation kinetics. The oxidation of the ceramic composites is diffusion controlled and the activation energies of oxygen in the oxide scale of the ceramics oxidized under temperatures below 1500 °C are 5134 J/mol and 5960 J/mol for ZS2 and ZS3, respectively. And ZS3 ceramics show better oxidation resistance. Then the oxidation of the material transforms to reaction controlled under elevated temperature due to evaporation of silica glass.

Acknowledgment

Thanks for the support from The Cheung Kong Scholars and Innovative Research Team Program in University from Ministry of Education of China (Grant no. IRT0805).

References

[1] M.M. Opeka, I.G. Talmy, J.A. Zaykoski, Oxidation-based materials selection for 2000 °C+hypersonic aero surfaces: theoretical considerations and historical experience, Journal of Materials Science 39 (2004) 5887–5904.
[2] K. Upadhya, J.M. Yang, W.P. Hoffmann, Materials for ultrahigh temperature structural applications, American Ceramic Society Bulletin 76 (1997) 51–56.
[3] Shu-Qi Guo, Jenn-Ming Yang, Hidehiko Tanaka, Yutaka Kagawa, Effect of thermal exposure on strength of ZrB_2-based composites with nano-sized SiC particles, Composites Science and Technology 68 (2008) 3033–3040.
[4] M.M. Opeka, I.G. Talmy, E.J. Wuchina, et al., Mechanical, thermal and oxidation properties of refractory hafnium and zirconium compounds, Journal of the European Ceramic Society 19 (1999) 2405–2414.
[5] C. Mroz, Zirconium diboride, American Ceramic Society Bulletin 73 (1994) 141–142.
[6] F. Monteverde, S. Guicciardi, A. Bellosi, Advances in microstructure and mechanical properties of zirconium diboride based ceramics, Materials Science and Engineering: A 346 (2003) 310–319.
[7] V. Milman, B. Winkler, M. I J Probert, Stiffness and thermal expansion of ZrB_2: an *ab initio* study, Journal of.Physics: Condensed Matter 17 (2005) 2233–2241.
[8] Weijie Li, Yong Zhang, Xinghong Zhang, et al., Thermal shock behavior of ZrB_2–SiC ultra-high temperature ceramics with addition of zirconia, Journal of Alloys and Compounds 478 (2009) 386–391.
[9] R.F. Voitovich, E.A. Pugach, High-temperature oxidation of the group IV metals: II. Oxidation of zirconium and hafnium diboride, Poroshkovaya Metallurgiya 3 (1975) 70–75.
[10] R.F. Voitovich, A. Pugach, L.A. Men'shikova, High temperature oxidation of ZrB_2, Poroshkovaya Metallurgiya 6 (1967) 44–48.
[11] Jiecai Han, Ping Hu, Xinghong Zhang, et al., Oxidation-resistant ZrB_2–SiC composites at 2200 °C, Composites Science and Technology 68 (2008) 799–806.
[12] D. Sciti, M. Brach, A. Bellosi, Long-term oxidation behavior and mechanical strength degradation of a pressurelessly sintered ZrB_2–$MoSi_2$ ceramic, Scripta Materialia 53 (2005) 1297–1302.
[13] F. Monteverde, A. Bellosi, Oxidation of ZrB_2-based ceramics in dry air, Journal of the Electrochemical Society 150 (2003) 552–559.

[14] A. Rezaie, William G. Fahrenholtz, Gregory E. Hilmas, Evolution of structure during the oxidation of zirconium diboride–silicon carbide in air up to 1500 °C, Journal of the European Ceramic Society 27 (2007) 2495–2501.
[15] William G. Fahrenholtz, Thermodynamic analysis of ZrB_2–SiC oxidation: formation of a SiC-depleted region, Journal of the American Ceramic Society 90 (2007) 143–148.
[16] T.A. Parthasarathy, R.A. Rapp, M. Opeka, R.J. Kerans, Modeling oxidation kinetics of SiC-containing refractory diborides, Journal of the American Ceramic Society 95 (1) (2012) 338–349.
[17] P. Sarin, P.E. Driemeyer, R.P. Haggerty, et al., In situ studies of oxidation of ZrB_2 and ZrB_2–SiC composites at high temperature, Journal of the European Ceramic Society 30 (11) (2010) 2375–2386.
[18] T. Tian, C. Zhou, F. Sun, et al., Oxidation kinetics of ZrB_2–SiC composites, Key Engineering Materials 368–372 (2008) 1750–1752.
[19] D. Gao, Y. Zhang, J. Fu, et al., Oxidation of zirconium diboride–silicon carbide ceramics under an oxygen partial pressure of 200 pa: formation of zircon, Corrosion Science 52 (10) (2010) 3297–3303.
[20] S.N. Karlsdottir, J.W. Halloran, A.N. Grundy, Zirconia transport by liquid convection during oxidation of zirconium diboride–silicon carbide, Journal of the American Ceramic Society 91 (2008) 272–277.
[21] Ju Li, Thomas J. Lenosky, Clemens J. Först, Sidney Yip, Thermochemical and mechanical stabilities of the oxide scale of ZrB_2–SiC and oxygen transport mechanisms, Journal of the American Ceramic Society 61 (2008) 1475–1480.
[22] Kuo-Chih Chou, Xin-Mei Hou, Kinetics of high-temperature oxidation of inorganic nonmetallic materials, Journal of the American Ceramic Society 82 (3) (2009) 585–594.
[23] X.M. Hou, K.-C. Chou, Quantitative interpretation of the parabolic and nonparabolic oxidation behavior of nitride ceramics, Journal of the European Ceramic Society 29 (2009) 517–523.
[24] Kuo-Chih Chou, A kinetic model for oxidation of Si–Al–O–N materials, Journal of the American Ceramic Society 89 (5) (2006) 1568–1576.
[25] X.M. Hou, K.C. Chou, Comparison of the diffusion control models for isothermal oxidation of Si–Al–O–N powders, Journal of the American Ceramic Society 91 (10) (2008) 3315–3319.